Terminal Phosphinidene Complexes $Cp^R(L)M{=}PAr$ of the Group 9 Transition Metals Cobalt, Rhodium, and Iridium. Synthesis, Structures, and Properties

Arjan T. Termaten,† Halil Aktas,† Marius Schakel,† Andreas W. Ehlers,† Martin Lutz,‡ Anthony L. Spek,‡ and Koop Lammertsma*,†

Department of Organic and Inorganic Chemistry, Faculty of Sciences, Vrije Universiteit, De Boelelaan 1083, NL-1081 HV, Amsterdam, The Netherlands, and Bijvoet Center for Biomolecular Research, Department of Crystal and Structural Chemistry, Utrecht University, Padualaan 8, NL-3584 CH, Utrecht, The Netherlands

Received October 15, 2002

Novel terminal rhodium- and cobalt-complexed phosphinidenes, $Cp^*(PR_3)Rh{=}PAr$ (**3**−**5**) and $Cp(PPh_3)Co{=}PAr$ (**8**), were obtained by dehydrohalogenation of the primary phosphine complexes $Cp^*RhCl_2(PH_2Ar)$ (**2**) and $CpCoI_2(PH_2Ar)$ (**7**) in the presence of a phosphine. X-ray crystal structures are reported for $Cp^*(PPh_3)Rh{=}PMes^*$ (**3**) and $Cp(PPh_3)Co{=}PMes^*$ (**8**). A comparative reactivity study and a computational survey were performed on the Co-, Rh-, and Ir-containing phosphinidene complexes. All react with organic dihalides to form phosphaalkenes, with the rhodium congener being far more reactive than the iridium and cobalt complexes. Density functional theory calculations give geometrical parameters and ^{31}P NMR chemical shifts in good agreement with experimental data. The rhodium congeners exhibit the most pronounced charge separation of the Rh=P bond, which may explain its higher reactivity. The M−L bond is strong in all Cp(L)M=PH (M = Co, Rh, Ir) complexes and inhibits reactivity at the metal center. Comparisons with the Zr-containing complex $Cp_2(PH_3)Zr{-}PH$ are made.

Introduction

Transition metal complexed phosphinidenes, $L_nM{=}PR$, are underdeveloped compared to the analogous carbene and imido complexes.[1] Despite the diagonal C−P relationship in the periodic table only a few well-characterized stable phosphinidene complexes are known. Most of these are nucleophilic and contain an early to middle transition metal of the second or third row.[2,3] Only few are known with late transition metals. The cationic complex $[Cp^*(CO)_2Ru{=}PN(^iPr)_2]^+$, recently prepared by Carty et al.,[4] represents a unique example of a stable electrophilic complex, and Hillhouse et al.[5] reported a nickel complex, (dtbpe)Ni=P(Dmp) (Dmp = 2,6-dimesitylphenyl; dtbpe = 1,2-bis(di-*tert*-butylphosphino)ethane), which is the first example of a fully characterized first-row transition metal complex.

Recently, we described highly stable iridium complexes of the type $Cp^*(L)Ir{=}PAr$ (L = PR_3, POR_3, AsR_3, dppe, RN≡C, and CO and Ar = Mes, Is, and Mes*),[6] which were generated by dehydrohalogenation of primary phosphine complex $Cp^*IrCl_2(PH_2Ar)$ with 1,8-diazabicyclo[5.4.0]undec-7-ene (DBU) in the presence of a stabilizing ligand (L). In this paper we describe the synthesis and characterization of phosphinidene complexes containing the other transition metals of group 9, namely, rhodium and cobalt. Furthermore, we present density functional theory (DFT) calculations on model complexes to demonstrate the role of the triad of metals (Co, Rh, Ir) and their stabilizing ligands on the philicity and reactivity of the phosphinidene complexes. In this analysis comparisons with the well-explored Zr-complexed phosphinidenes are made to highlight differences in electronic properties.

Results and Discussion

The synthesis and characterization of novel rhodium and cobalt phosphinidene complexes are described first, followed by a discussion on their reactivity with the assistance of density functional theory calculations.

A. Synthesis of $Cp^*(PR_3)Rh{=}PAr$. The precursors in our approach are the rhodium-complexed primary phosphines $Cp^*RhCl_2(PH_2Ar)$ (**2a**,**b**), which are readily prepared in high yields (86−94%) from commercially available $[Cp^*RhCl_2]_2$ (**1**) and phosphines (Scheme 1) that contain either the bulky supermesityl (Mes*; 2,4,6-tri-*tert*-butylphenyl) group or the less congesting isityl

* Corresponding author. Tel: + 31-20-444-7474. Fax: + 31-20-444-7488. E-mail: lammert@chem.vu.nl.
† Vrije Universiteit.
‡ Utrecht University.

(1) Mathey, F.; Tran Huy, N. H.; Marinetti, A *Helv. Chim. Acta* **2001**, *84*, 2938. (b) Lammertsma, K.; Vlaar, M. J. M. *Eur. J. Org. Chem.* **2002**, *4*, 1127.
(2) Cowley, A. H.; Barron, A. R. *Acc. Chem. Res.* **1988**, *21*, 81. (b) Cowley, A. H. *Acc. Chem. Res.* **1997**, *30*, 445.
(3) Dillon, K. B.; Mathey, F.; Nixon, J. F. *Phosphorus: The Carbon Copy*; Wiley: Chichester, 1998; Chapter 3.
(4) Sterenberg, B. T.; Carty, A. J. *J. Organomet. Chem.* **2001**, *617*−*618*, 696. (b) Sterenberg, B. T.; Udachin, K. A.; Carty, A. J. *Organometallics* **2001**, *20*, 2657. (c) Sterenberg, B. T.; Udachin, K. A.; Carty, A. J. *Organometallics* **2001**, *20*, 4463.
(5) Melenkivitz, R.; Mindiola, D. J.; Hillhouse, G. L. *J. Am. Chem. Soc.* **2002**, *124*, 3846.
(6) Termaten, A. T.; Nijbacker, T.; Schakel, M.; Lutz, M.; Spek, A. L.; Lammertsma, K. *Organometallics* **2002**, *21*, 3196.

10.1021/om0208624 CCC: $25.00
Publication on Web 04/02/2003

Scheme 1

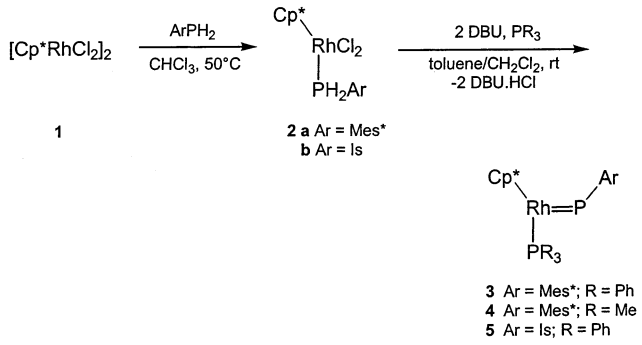

(Is; 2,4,6-tri-isopropylphenyl) group. The ^{31}P NMR spectra of **2a**,**b** show large diagnostic $^{1}J_{PH}$ coupling constants of ~387 Hz and typical $^{1}J_{RhP}$ values of ~140 Hz.[7]

Phosphinidene complexes are then obtained from **2a**,**b** in a dehydrohalogenation−ligation sequence. For example, addition of a CH_2Cl_2 solution of **2a** to a solution of DBU and PPh_3 in toluene at room temperature affords dark green colored terminal rhodium complex **3** (Scheme 1) in high yield (89%). The low-field ^{31}P NMR resonance at δ 868 and the small $^{1}J_{RhP}$ coupling constant of 69 Hz are characteristic for a bent phosphinidene.[2b,3] Its considerable downfield shift with respect to the heavier iridium analogue (δ 687)[6] relates to a similar difference in chemical shifts between the molybdenum (δ 800) and tungsten (δ 661) complexes of Cp_2M=PMes*.[8] The large $^{1}J_{RhP}$ coupling constant of 239 Hz for the phosphine resonance at δ 44 suggests a strong Rh−PPh_3 bonding interaction.

The structure of **3**, ascertained by an X-ray determination (Figure 1), is similar to that of the previously described iridium analogue.[6] It has a two-legged piano stool arrangement with a short Rh(1)−P(1) double bond of 2.1903(4) Å, a Rh(1)−P(2) single bond of 2.2647(4) Å, and an acute P(1)−Rh(1)−P(2) angle of 86.524(15)°. The steric congestion in the system is evident from the nonplanarity of the Mes* ring with a maximum torsion angle of 13.8(2)° in the ring. The *E* configuration for the Rh=P double bond is consistent with the observed large $^{2}J_{PP}$ coupling constant of 59 Hz; *Z* isomers have smaller $^{2}J_{PP}$ values and an even more deshielded δ(^{31}P) for the phosphinidene group.[6]

The same dehydrohalogenation−ligation sequence, but using the smaller PMe_3 ligand instead of PPh_3, yielded Cp*(PMe_3)Rh=PMes* (**4**) as a mixture of *E* and *Z* isomers (35:65) in a combined yield of 79%. The ^{31}P NMR spectrum of the *E* isomer exhibits double doublets at δ 815 ($^{1}J_{RhP}$ = 66 Hz) and −14 ($^{1}J_{RhP}$ = 232 Hz), both with a $^{2}J_{PP}$ coupling constant of 35 Hz. The *Z* isomer shows the expected deshielding for the phosphinidene resonance (δ 953; $^{1}J_{RhP}$ = 86 Hz) and a decrease in $^{2}J_{PP}$ (19 Hz), but a similar phosphine chemical shift at δ −7 ($^{1}J_{RhP}$ = 230 Hz). Dehydrohalogenation of Cp*$RhCl_2$-(PH_2Is) (**2b**) in the presence of PPh_3 afforded in 82% yield only (*E*)-Cp*(PPh_3)Rh=PIs (**5**), the assignment of which is based on its chemical shifts at δ 859 ($^{1}J_{RhP}$ = 63 Hz) and 45 ($^{1}J_{RhP}$ = 234 Hz) and $^{2}J_{PP}$ coupling constant of 38 Hz.

The stability of the complexes decreases rapidly with less crowded aromatic rings such as Mes and with smaller metal ligands such as CO. For example, dehydrohalogenation of Cp*$RhCl_2$(PH_2Mes) in the presence of PPh_3 gave in low yield (~10%) (*E*)-Cp*(PPh_3)-Rh=PMes, which could only be detected by its ^{31}P NMR chemical shifts at δ 845 and 47 and their characteristic $^{2}J_{RhP}$ coupling constants of 65 and 232 Hz, respectively. Introduction of a carbonyl ligand, by leading CO through the reaction mixture during the dehydrohalogenation of **2a**, led only to intractable material in contrast to the same procedure that was reported to give the stable iridium analogue Cp*(CO)Ir=PMes*.[6] This suggests that access to rhodium phosphinidene complexes is more limited than is the case for the iridium analogues. The imido complexes appear to behave likewise, as iridium complexes Cp*Ir≡N−R are stable isolable compounds, while the rhodium analogues have so far remained elusive.[9,10]

B. Synthesis of Cp*(PR_3)Co=PAr. The dehydrohalogenation−ligation sequence that was used for the Ir and Rh phosphinidene complexes proved to be more difficult for the cobalt complexes. Even the synthesis of precursors was problematic, but $CpCoI_2$(Mes*PH_2) (**7**) could be prepared successfully from $[CpCoI_2]_n$ (**6**) and Mes*PH_2 in 78% yield as a dark green solid (Scheme 2), even though it decomposes slowly in solution. Its ^{31}P NMR spectrum shows a characteristic broad triplet at δ −49 with a large $^{1}J_{PH}$ of 382 Hz.

Addition of a CH_2Cl_2 solution of **7** to a solution of DBU and PPh_3 in toluene at 0 °C led to the formation of dark red phosphinidene complex **8** (Scheme 2). The limited yield (42%) is due to a competing ligand exchange that leads to the more stable Cp(PPh_3)CoI_2 [11] and Mes*PH_2. This side reaction could not be suppressed and illustrates that Mes*PH_2 is only weakly coordinated in **7**, which contributes to its instability in solution.

The ^{31}P NMR spectrum of **8** shows resonances at δ 867 and 54 for the phosphinidene and phosphine groups, respectively. Both are broad due to the high nuclear spin (7/2) and large electric quadrupole moment of the ^{59}Co nucleus. The $^{2}J_{PP}$ coupling constant of 76 Hz suggests an *E* configuration for the Co=P bond, which was confirmed by an X-ray crystal structure determination (Figure 2). The two-legged piano stool geometry has a short Co(1)−P(1) bond of 2.1102(8) Å, which illustrates its double-bond character. The 2.1893(8) Å Co(1)−P(2) bond distance is normal for a Co−PPh_3 single bond, which ranges from 2.15 to 2.23 Å.[12] The P(1)−Co(1)−P(2) angle of 89.96(3)° is less acute than those of the rhodium and iridium analogues, which may have its origin in the increased steric congestion that is caused by the shorter metal−ligand bonds of the cobalt complex.

Using CO as stabilizing ligand instead of PPh_3 resulted in cobalt phosphinidene complex (*Z*)-Cp(CO)-Co=PMes*, as indicated by its ^{31}P NMR resonance at δ

(7) Esteban, M.; Pequerul, A.; Carmona, D.; Lahoz, F. J.; Martín, A.; Oro, L. A. *J. Organomet. Chem.* **1991**, *402*, 421.
(8) Hitchcock, P. B.; Lappert, M. F.; Leung, W. P. *J. Chem. Soc., Chem. Commun.* **1987**, 1282.
(9) Glueck, D. S.; Wu, J.; Hollander, F. J.; Bergman, R. G. *J. Am. Chem. Soc.* **1991**, *113*, 2041.
(10) Danopoulos, A. A.; Wilkinson, G.; Sweet, T. K. N.; Hursthouse, M. B. *J. Chem. Soc., Dalton Trans.* **1996**, 3771.
(11) King, R. B. *Inorg. Chem.* **1966**, *5*, 82. (b) Roe, D. M.; Maitlis, P. M. *J. Chem. Soc. (A)* **1971**, 3173.
(12) Wakatsuki, Y.; Sakurai, T.; Yamazaki, H. *J. Chem. Soc., Dalton Trans.* **1982**, 1923. (b) Diversi, P.; Ingrosso, G.; Lucherini, A.; Porzio, W.; Zocchi, M. *Chem. Commun.* **1977**, 811.

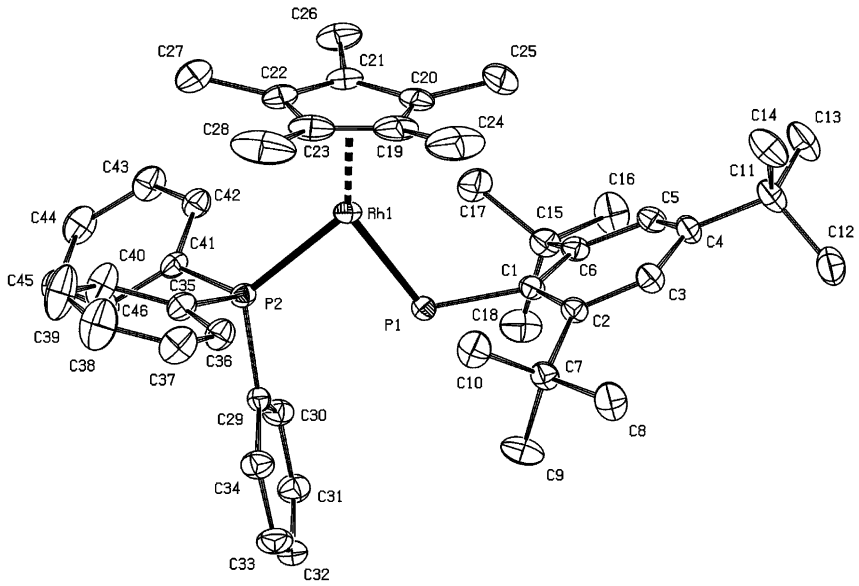

Figure 1. Displacement ellipsoid plot (50% probability level) of **3**. Hydrogen atoms are omitted for clarity. Selected bond distances (Å), angles (deg), and torsion angles (deg): Rh(1)−P(1) 2.1903(4), Rh(1)−P(2) 2.2647(4), Rh(1)−Cp(cg) 1.9253(9), P(1)−C(1) 1.8503(16), P(2)−C(29) 1.8374(16), P(2)−C(35) 1.8321(17), P(2)−C(41) 1.8411(16), Rh(1)−P(1)−C(1) 113.94(5), P(1)−Rh(1)−Cp(cg) 143.25(3), P(1)−Rh(1)−P(2) 86.524(15), P(2)−Rh(1)−Cp(cg) 130.20(3), C(6)−C(1)−C(2)−C(3) 13.8(2), C(2)−C(1)−C(6)−C(5) −13.2(2).

Scheme 2

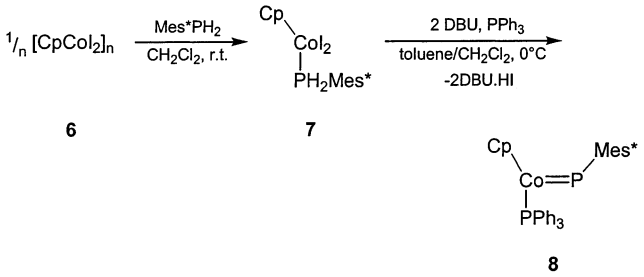

1047, but its yield (∼10%) is too low to be isolated. The more congested Cp* analogue of phosphinidene precursor **7**, i.e., $Cp^*CoI_2(PH_2Mes^*)$ (**9**) ($\delta(^{31}P)$ −86, $^1J_{PH} = 394$ Hz), was too unstable to sustain the dehydrohalogenation−ligation procedure.

C. Reactivity of Group 9 Phosphinidene Complexes. NMR-scale experiments were conducted to compare the reactivities of Rh complex **3** and Co complex **8** with those of the previously reported Ir complexes.[6] All three systems behave similarly, but there are subtle differences. For example, Rh complex **3** reacts faster than the others with organic halides, such as CH_2X_2 and CHX_3 (X = Cl, Br, I), to give phosphaalkenes and $Cp^R(PPh_3)MX_2$. Reaction of **3** with CH_2I_2 in pentane proceeds within 1 h quantitatively at room temperature, whereas it takes several days at 60 °C for the iridium analogue. Moreover, **3** reacts also with CH_2Br_2 and CH_2Cl_2 in decreasing order. The reactivity of **3** increases by reducing the size of its stabilizing ligand PR_3.

Neither of the Co, Rh, and Ir complexed phosphinidenes undergo "phospha-Wittig" reactions[2b,13] with carbonyl groups nor do they give [1 + 2] cycloadditions with olefins or alkynes. This behavior contrasts that of both the established nucleophilic $Cp_2(PMe_3)Zr{=}PMes^*$[14] and the electrophilic $(CO)_5W{=}PR$ and $(CO)_4Fe{=}PN^iPr_2$.[1−3,15] To address the electronic and steric influences of the group 9 phosphinidene complexes in relationship to the Zr complex, we resorted to DFT calculations on model systems.

D. Theoretical Calculations. In a recent study on a series of transition metal complexed phosphinidenes, Ehlers et al.[16] showed that their philicity is largely determined by the ancillary ligands of the metal rather than by the metal itself. This electronic effect results from charge transfer between the transition metal ligands and the phosphorus atom. It can then be argued that the group 9 phosphinidene complexes are ambiphilic. Namely, they carry a single π-accepting Cp* ligand besides an electron-donating phosphine group, which distinguishes them, for example from the nucleophilic $Cp_2(PMe_3)Zr{=}PMes^*$[14] and the electrophilic $(CO)_5W{=}PR$.[1,3,17]

To evaluate the properties of the group 9 phosphinidene complexes, we performed DFT calculations on the unsubstituted model system, using Cp, CO, and PH_3 as metal ligands. We start by discussing structural and magnetic properties, followed by an analysis of metal−ligand bond energies and atomic charges.

Geometries and ^{31}P NMR Chemical Shifts. As model Co, Rh, and Ir systems we use (*E*/*Z*)-$Cp(PH_3)$-M=PH and (*E*/*Z*)-Cp(CO)M=PH. Their optimized geometries (C_s symmetry) are depicted for M = Ir in Figure 3. All *E*/*Z* relative energies, selected bond distances, and angles are collected in Table 1. The calculated geometries show good agreement with the X-ray crystal structures of **8** (Co), **3** (Rh), $Cp^*(PPh_3)Ir{=}PMes^*$,

(13) Shah, S.; Protasiewicz, J. D. *Coord. Chem. Rev.* **2000**, *210*, 181.
(14) Breen, T. L.; Stephan, D. W. *J. Am. Chem. Soc.* **1995**, *117*, 11914.
(15) Wit, J. B. M.; van Eijkel, G. T.; de Kanter, F. J. J.; Schakel, M.; Ehlers, A. W.; Lutz, M.; Spek, A. L.; Lammertsma, K. *Angew. Chem.* **1999**, *111*, 2716; *Angew. Chem., Int. Ed.* **1999**, *38*, 2596. (b) Wit, J. B. M.; van Eijkel, G. T.; Schakel, M.; Lammertsma, K. *Tetrahedron* **2000**, *56*, 137.
(16) Ehlers, A. W.; Baerends, E.-J.; Lammertsma, K. *J. Am. Chem. Soc.* **2002**, *124*, 2831.
(17) Mathey, F. *Angew. Chem.* **1987**, *99*, 285−296; *Angew. Chem., Int. Ed. Engl.* **1987**, *26*, 275.

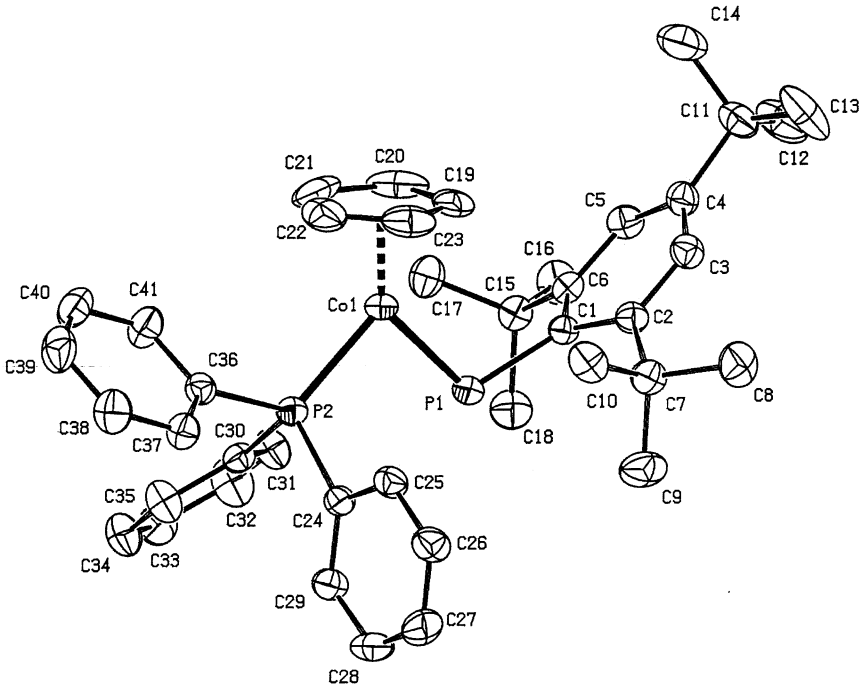

Figure 2. Displacement ellipsoid plot (50% probability level) of $Cp(PPh_3)Co{=}PMes^*{\cdot}C_5H_{12}$ (**8**). *n*-Pentane and the hydrogen atoms are omitted for clarity. Selected bond distances (Å), angles (deg), and torsion angles (deg): Co(1)−P(1) 2.1102(8), Co(1)−P(2) 2.1893(8), Co(1)−Cp(cg) 1.7159(19), P(1)−C(1) 1.861(3) Å, P(2)−C(24) 1.828(3), P(2)−C(30) 1.842(4), P(2)−C(36) 1.838(3), Co(1)−P(1)−C(1) 109.00(9), P(1)−Co(1)−Cp(cg) 136.74(7), P(1)−Co(1)−P(2) 89.96(3), P(2)−Co(1)−Cp(cg) 132.99(7), C(6)−C(1)−C(2)−C(3) 15.7(4), C(2)−C(1)−C(6)−C(5)−16.4(4).

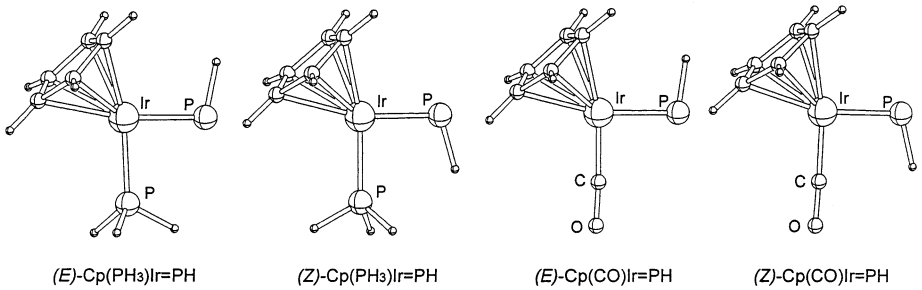

Figure 3. DFT optimized structures (C_s symmetry) for Cp(CO)Ir=PH and $Cp(PH_3)Ir{=}PH$.

Table 1. Calculated Relative Energies[a] (kcal/mol) and Selected Bond Distances (Å) and Angles (deg) for (*E*)- and (*Z*)-Cp(L)M=PH (L = CO, PH_3; M = Co, Rh, Ir)

complex	energy	M=P	M−L	Cp-M	Cp-M=P	M=P−H	L−M=P
(*E*)-Cp(CO)Co=PH	+2.75	2.105	1.741	1.714	134.7	99.4	90.5
(*Z*)-Cp(CO)Co=PH	0.00	2.090	1.723	1.724	131.9	106.7	90.7
(*E*)-Cp(PH_3)Co=PH	+0.34	2.095	2.137	1.690	136.8	101.9	90.4
(*Z*)-Cp(PH_3)Co=PH	0.00	2.089	2.113	1.706	132.7	107.1	91.6
(*E*)-Cp(CO)Rh=PH	+2.10	2.215	1.869	1.949	135.6	97.9	88.2
(*Z*)-Cp(CO)Rh=PH	0.00	2.206	1.858	1.957	133.1	105.7	88.9
(*E*)-Cp(PH_3)Rh=PH	+0.43	2.202	2.251	1.928	137.9	100.9	86.7
(*Z*)-Cp(PH_3)Rh=PH	0.00	2.195	2.230	1.949	134.4	106.8	88.8
(*E*)-Cp(CO)Ir=PH	+1.30	2.229	1.858	1.969	135.4	98.4	89.3
(*Z*)-Cp(CO)Ir=PH	0.00	2.220	1.848	1.976	132.0	105.2	91.2
(*E*)-Cp(PH_3)Ir=PH	−0.46	2.218	2.239	1.942	138.4	101.4	86.8
(*Z*)-Cp(PH_3)Ir=PH	0.00	2.213	2.226	1.957	134.5	106.2	90.1

[a] The energy of the *E* isomer relative to its *Z* isomer (0.00 kcal/mol).

and Cp*(CO)Ir=PMes*.[6] Only the M=P−H angles are underestimated by 7−13°, which is attributed to the absence of steric congestion in the model structures.[19] The *E* and *Z* isomers for each of the model complexes have similar energies, which agrees with those experiments in which both isomers were obtained. Steric congestion is considered to be the determining factor for formation of the *E* isomer, as it tends to be slightly less stable.

The *E*/*Z* configuration of the M=P bond hardly effects the geometrical parameters, but it has a profound impact on the ^{31}P NMR chemical shifts. This is a well-known characteristic of phosphaalkenes and is related

(18) Goede, S. J.; van Schaik, H. P.; Bickelhaupt, F. *Organometallics* **1992**, *11*, 3844.
(19) Pyykkö, P. *Chem. Rev.* **1988**, *88*, 563.

Table 2. Theoretical ^{31}P NMR Isotropic Shielding Tensors, Chemical Shifts (ppm), and $^2J_{PP}$ Coupling Constants for Complexed Phosphinidenes

complex	isotropic shielding	δ (^{31}P) calcd[a]	$^2J_{PP}$ calcd	δ ^{31}P ($^2J_{PP}$) expt
(*E*)-$Cp(PH_3)Co{=}PH$	−611.6	+903	207	867 (76)[b]
(*Z*)-$Cp(PH_3)Co{=}PH$	−686.3	+977	66	
(*E*)-$Cp(PH_3)Rh{=}PH$	−603.3	+894	171	868 (59)[c]
				815 (35)[d]
(*Z*)-$Cp(PH_3)Rh{=}PH$	−650.8	+942	30	953 (19)[d]
(*E*)-$Cp(PH_3)Ir{=}PH$	−437.5	+729	216	687 (102)[c]
				629 (84)[d]
(*Z*)-$Cp(PH_3)Ir{=}PH$	−476.9	+768	21	727 (18)[d]
(*E*)-Cp(CO)Co=PH	−715.4	+1006		
(*Z*)-Cp(CO)Co=PH	−752.7	+1044		1047[e]
(*E*)-Cp(CO)Rh=PH	−708.8	+1000		
(*Z*)-Cp(CO)Rh=PH	−730.4	+1022		
(*E*)-Cp(CO)Ir=PH	−538.2	+829		
(*Z*)-Cp(CO)Ir=PH	−552.9	+844		805[f]

[a] Relative to PMe_3 (δ −62 with respect to 85% H_3PO_4). [b] (*E*)-[Cp(PPh$_3$)Co=PMes*]. [c] (*E*)-[Cp*(PPh$_3$)M=PMes*] (M = Rh, Ir). [d] (*E*/*Z*)-[Cp*(PMe$_3$)M=PMes*] (M = Rh, Ir). [e] [Cp(CO)Co=PMes*]. [f] [Cp*(CO)Ir=PMes*].

to the environment of the lone pair on phosphorus.[18] The DFT calculated ^{31}P NMR isotropic shielding tensors and chemical shifts (referenced against PMe_3) and, where applicable, $^2J_{PP}$ coupling constants are listed in Table 2. The chemical shifts compare remarkably well with those observed experimentally, considering the tremendous difference in steric bulk, and thereby support the assignment of the more deshielded ^{31}P NMR chemical shift to the *Z* isomer. The difference in $\Delta\delta$ for the *E* and *Z* isomers decreases in the order Co > Rh > Ir, as is also observed. The phosphinidene chemical shifts of the Ir complexes are shielded as compared to the Rh complexes, and these are again more shielded than those of the Co complexes, which reflects a heavy metal effect.[19] Also the transition metal ligands influence the chemical shift of the =P-phosphorus, with that of the CO-ligated structure being the most deshielded one for each of the metal complexes. Last, the $^2J_{PP}$ coupling constants for the PH_3-ligated complexes are larger for the *E* than for the *Z* forms, although the applied DFT method appears to significantly overestimate the absolute values.

Bond Energies and Atomic Charges. Stable nucleophilic phosphinidene complexes, including those of group 9, may well be hampered in their reactivity by steric congestion of both their ligands and substituents. However, this is contrasted by the reported reactions of the bulky $Cp_2(PMe_3)Zr{=}PAr$ (Ar = Mes* (**10a**), Dmp (**10b**)) with various substrates including carbonyl compounds and organic halides.[14,20] This apparent discrepancy requires closer scrutiny.

A distinguishing feature of **10** is the ease by which it loses or exchanges the phosphine ligand, thereby suggesting that the active species may, in fact, be the 16-electron complex $Cp_2Zr{=}PAr$. For example, reaction of **10** with a carbonyl group presumably proceeds via initial coordination of the oxygen to the metal (with loss of PMe_3), followed by nucleophilic attack of the phosphinidene on the carbonyl carbon to form a Zr−P−C−O cyclic intermediate. Retrocyclization then affords $[Cp_2ZrO]_n$ and a phosphaalkene.[14] We note that the $M{-}PH_3$ distance is 0.24 Å longer than the M=P bond in **10a**, whereas this difference amounts to only 0.04−0.07 Å for the group 9 phosphinidene complexes **3**, **8**, and Cp*(PPh$_3$)Ir=Pmes*. Evidently, the phosphine ligand is more tightly bound to the metal in the group 9 complexes, indicating that the intermediate formation of a 16-electron species is not likely. The calculated metal−ligand bond dissociation energies (BDEs), listed in Table 3, seem to support this notion. The BDE for the $M{-}PH_3$ bond of $Cp_2(PH_3)Zr{=}PH$ amounts to only 22.2 kcal/mol, whereas those of both the *E* and *Z* isomers of the Co and Rh complexes are much higher, with an average value of 34 kcal/mol, and those of the Ir complexes are higher still (42 kcal/mol). The $\Delta E_{A'}$ (σ) and $\Delta E_{A''}$ (π) contributions to the orbital interaction energy (ΔE^{oi}) confirm PH_3 to act as a strong σ-donor/weak π-acceptor ligand in $Cp(PH_3)M{=}PH$, as expected.[21,22] The CO ligands are more tightly bound to the metal with 11.9−18.8 kcal/mol larger BDEs due to their stronger π-acceptor abilities, i.e., ΔE_σ amounts to 60−70% of ΔE_π.[23,24] The BDEs of the M−CO bonds follow the Co ≈ Rh < Ir order. The iridium complexes are the most tightly ligated ones due to stronger σ-donation, which is caused by relativistic effects that are known to be more important for the third-row transition metals.[19]

The key distinguishing feature of the phosphinidene complexes, however, is their philicity, which is determined by the relative charge on the phosphorus atoms as explored earlier by Ehlers et al.[16] In Table 4, the calculated Hirshfeld charges[25] for both the metal and the phosphinidene phosphorus atoms are listed for all Co, Rh, and Ir complexes together with those of $Cp_2(PH_3)Zr{=}PH$.[26] It is evident that the negative charge on phosphorus decreases upon changing the PH_3 ligand in Cp(L)M=PH for Co due to the difference in π-acceptor abilities.[16] Within the nucleophilic PH_3-ligated series, the Rh complexes have a much more polarized M=P bond than both the Co and Ir congeners, even though the polarization is far less than the Zr=P bond in $Cp_2(PH_3)Zr{=}PH$. We presume that this charge separation is an important factor in the affinity of the phosphinidene complexes for other polarized bonds such as the C−Cl bonds in the dihalides. This would explain why the Rh-containing complexes are the most reactive of the group 9 series but still far less reactive than $Cp_2(PMe_3)Zr{=}PAr$.

Conclusions

In this paper, the synthesis and characterization of novel terminal rhodium and cobalt phosphinidene complexes are described. Their synthesis involves dehydro-

(20) Urnezius, E.; Shah, S.; Protasiewicz, J. D. *Phosphorus, Sulfur Silicon* **1999**, *144*−*146*, 137. (b) Urnezius, E.; Lam, K.-C.; Rheingold, A. L.; Protasiewicz, J. D. *J. Organomet. Chem.* **2001**, *630*, 193.

(21) Frenking, G.; Wichman, K.; Fröhlich, N.; Grobe, J.; Golla, W.; Le Van, D.; Krebs, B.; Läge, M. *Organometallics* **2002**, *21*, 2921−2930.

(22) Gonzáles-Blanco, O.; Branchadell, V. *Organometallics* **1997**, *161*, 5556−5562.

(23) Frenking, G.; Fröhlich, N. *Chem. Rev.* **2000**, *100*, 717−774.

(24) Ehlers, A. W.; Ruiz-Morales, Y.; Baerends, E. J.; Ziegler, T. *Inorg. Chem.* **1997**, *360*, 5031−5036.

(25) Hirshfeld, F. L. *Theor. Chim. Acta* **1977**, *44*, 129. (b) Wiberg, K. B.; Rablen, P. R. *J. Comput. Chem.* **1993**, *14*, 1504.

(26) $Cp_2(PH_3)Zr{=}PH$] was calculated in a similar manner (C_1 symmetry) as all group 9 phosphinidenes. Some bond distances (Å) and angles (deg): Zr=P 2.502, Zr−P 2.682, Cp−Zr−Cp 137.1, P−Zr=P 82.4. Calculated ^{31}P NMR isotropic shielding tensor: −530.17 (δ 821 with respect to PMe_3; expt δ 792).

Table 3. Calculated Bond Energies and Bond Dissociation Energies (kcal/mol)[a] for M−L in [Cp(L)M=PH] and [$Cp_2(PH_3)$Zr=PH]

	$\Delta E_{A'}$	$\Delta E_{A''}$	ΔE_σ	ΔE_π	ΔE^{oi}	ΔE°	ΔE^{tot}	BDE
(*E*)-Cp(PH_3)Co=PH	−48.9	−13.5	−35.4	−27.0	−62.4	23.9	−38.5	33.5
(*Z*)-Cp(PH_3)Co=PH	−53.3	−13.9	−39.4	−27.8	−67.2	21.4	−45.8	33.8
(*E*)-Cp(PH_3)Rh=PH	−51.6	−13.9	−37.7	−27.8	−65.5	26.1	−39.4	34.4
(*Z*)-Cp(PH_3)Rh=PH	−53.2	−14.1	−39.1	−28.2	−67.3	21.1	−46.2	34.8
(*E*)-Cp(PH_3)Ir=PH	−72.1	−17.6	−54.5	−35.2	−89.7	36.4	−53.3	42.2
(*Z*)-Cp(PH_3)Ir=PH	−76.5	−17.7	−58.8	−35.4	−94.2	36.9	−57.2	41.8
(*E*)-Cp(CO)Co=PH	−66.6	−31.8	−34.8	−63.6	−98.4	41.4	−57.0	49.8
(*Z*)-Cp(CO)Co=PH	−69.9	−32.7	−37.2	−65.4	−102.6	36.3	−66.2	52.6
(*E*)-Cp(CO)Rh=PH	−72.6	−30.9	−41.7	−61.8	−103.5	49.6	−53.9	46.3
(*Z*)-Cp(CO)Rh=PH	−71.3	−31.5	−39.8	−63.0	−102.8	41.8	−61.0	48.4
(*E*)-Cp(CO)Ir=PH	−99.2	−39.1	−60.1	−78.2	−138.3	64.6	−73.7	58.3
(*Z*)-Cp(CO)Ir=PH	−100.9	−39.9	−61.0	−79.8	−140.8	62.1	−78.7	59.6
$Cp_2(PH_3)$Zr=PH[b]	n.d.[c]	n.d.[c]	n.d.[c]	n.d.[c]	−39.1	15.0	−24.1	22.2

[a] For definitions, see Computational Section. [b] See ref 21 for structural data. [c] Not determined due to low symmetry (C_1) of the system.

Table 4. Calculated Hirshfeld Charges of M and P in Cp(L)M=PH and $Cp_2(PH_3)$Zr=PH

complex	M	P
(*E*)-Cp(PH_3)Co=PH	−0.086	−0.066
(*Z*)-Cp(PH_3)Co=PH	−0.085	−0.056
(*E*)-Cp(PH_3)Rh=PH	+0.108	−0.111
(*Z*)-Cp(PH_3)Rh=PH	+0.107	−0.101
(*E*)-Cp(PH_3)Ir=PH	−0.027	−0.089
(*Z*)-Cp(PH_3)Ir=PH	−0.029	−0.087
(*E*)-Cp(CO)Co=PH	−0.038	+0.004
(*Z*)-Cp(CO)Co=PH	−0.036	+0.010
(*E*)-Cp(CO)Rh=PH	+0.163	−0.046
(*Z*)-Cp(CO)Rh=PH	+0.162	−0.045
(*E*)-Cp(CO)Ir=PH	+0.044	−0.021
(*Z*)-Cp(CO)Ir=PH	+0.042	−0.024
$Cp_2(PH_3)$Zr=PH	+0.333	−0.270

halogenation of the primary phosphine complexes Cp*$RhCl_2(PH_2Ar)$ (**2**) and $CpCoI_2(PH_2Mes^*)$ (**7**) by DBU in the presence of a stabilizing phosphine ligand. X-ray crystal structures are presented for Cp*(PPh_3)Rh=PMes* (**3**) and Cp(PPh_3)Co=PMes* (**8**), thereby completing the first (group 9) transition metal triad of phosphinidene complexes. All react with organic dihalides, with the rhodium congener being by far the most reactive one. No reactivity toward C=C, C≡C, and C=O bonds was observed.

DFT calculations on the model systems (*E*/*Z*)-Cp(PH_3)M=PH and (*E*/*Z*)-Cp(CO)M=PH show the geometrical parameters and ^{31}P NMR chemical shifts to be in good agreement with experimental data. Calculated Hirshfeld charges show the Rh=P bond to be much more polarized than the iridium and cobalt analogues, which explains their difference toward organic halides.

The M−L ligand bonds of the group 9 complexes Cp(L)M=PH are much stronger than that of $Cp_2(PH_3)$Zr=PH and make ligand exchange or loss an unlikely process. This, together with the low oxophilicity of the group 9 transition metals, makes these phosphinidene complexes unreactive toward carbonyl groups.

Computational Section

All calculations were performed using the parallelized Amsterdam density functional (ADF) package (version 2000.02).[27] All atoms were described by a triple-ζ basis set with polarization functions, corresponding to basis set IV in the ADF. The 1s core shell of carbon and oxygen and the 1s2s2p core shells of phosphorus were treated by the frozen core approximation. The metal centers were described by a triple-ζ basis set for the outer *n*s, *n*p, *n*d, and (*n* + 1)s orbitals, whereas the shells of lower energy were treated by the frozen core approximation. All calculations were performed at the nonlocal exchange self-consistent field (NL-SCF) level, using the local density approximation (LDA) in the Vosko−Wilk−Nusair parametrization[28] with nonlocal corrections for exchange (Becke88)[29] and correlation (Perdew86).[30] All geometries were optimized using the analytical gradient method implemented by Versluis and Ziegler,[31] including relativistic effects by the zero-order regular approximation (ZORA).[32]

The ^{31}P NMR chemical shift tensors were calculated with ADF's NMR program,[33] including an all-electron basis set and relativistic effects (ZORA) for the phosphorus atoms. All other atoms were treated as mentioned above. All model complexes were calculated without molecular symmetry. The total isotropic shielding tensors were referenced against PMe_3, which has a value of 353.08. It has an experimental chemical shift at δ −62 with respect to 85% H_3PO_4. The $^2J_{PP}$ coupling constants were calculated with a preliminary version of ADF's CCL program.[34]

The metal−ligand bonds were analyzed with ADF's established energy decomposition[35] into an exchange repulsion plus electrostatic interaction energy part (ΔE°) and an orbital interaction energy (charge transfer, polarization) part (ΔE^{oi}). The energy necessary to convert fragments from their ground-state equilibrium geometries to the geometry and electronic state they acquire in the complex is represented by a preparation energy term (ΔE^{prep}). The overall bond energy (ΔE^{tot}) is formulated as $\Delta E^{tot} = \Delta E^\circ + \Delta E^{oi} + \Delta E^{prep}$.

Note that ΔE^{tot} is defined as the negative of the bond dissociation energy (BDE), i.e., $\Delta E^{tot} = E(\text{molecule}) - \sum E(\text{fragments})$, thereby giving negative values for stable bonds. The orbital interaction term ΔE^{oi} accounts for charge transfer (interactions between occupied orbitals on one fragment with unoccupied orbitals on the other, including HOMO−LUMO

(27) te Velde, G.; Bickelhaupt, F. M.; van Gisbergen, S. J. A.; Fonseca Guerra, C.; Baerends, E. J.; Snijders, J. G.; Ziegler, T. Chemistry with ADF. *J. Comput. Chem.* **2001**, *22*, 931. (b) Fonseca Guerra, C.; Snijders, J. G.; te Velde, G.; Baerends, E. J. *Theor. Chem. Acc.* **1998**, *99*, 391. (c) ADF2000.02, SCM, Theoretical Chemistry, Vrije Universiteit, Amsterdam, The Netherlands, http://www.scm.com.

(28) Vosko, S. H.; Wilk, L.; Nusair, M. *Can. J. Phys.* **1992**, *70*, 84.

(29) Becke, A. D. *Phys. Rev. A* **1988**, *38*, 3098.

(30) Perdew, J. P. *Phys. Rev. B* **1986**, *33*, 8822.

(31) Fan, L.; Versluis, L.; Ziegler, T.; Baerends, E. J.; Raveneck, W. *Int. J. Quantum. Chem.; Quantum. Chem. Symp.* **1988**, *S22*, 173. (b) Versluis, L.; Ziegler, T. *Chem. Phys.* **1988**, *322*, 88.

(32) van Lenthe, E.; Ehlers, A. W.; Baerends, E. J. *J. Chem. Phys.* **1999**, *110*, 8943.

(33) Schreckenbach, G.; Ziegler, T. *J. Phys. Chem.* **1995**, *99*, 606−611. (b) Schreckenbach, G.; Ziegler, T. *Int. J. Quantum Chem.* **1997**, *61*, 899. (c) Wolff, S. K.; Ziegler, T. *J. Chem. Phys.* **1998**, *109*, 895.

(34) Autschbach, J.; Ziegler, T *J. Chem. Phys.* **2000**, *113*, 936. (b) Autschbach, J.; Ziegler, T *J. Chem. Phys.* **2000**, *113*, 9410.

(35) Morokuma, K. *Acc. Chem. Res.* **1977**, *10*, 297. (b) Ziegler, T.; Rauk, A. *Inorg. Chem.* **1979**, *18*, 1755. (c) Ziegler, T.; Rauk, A. *Theor. Chim. Acta* **1977**, *46*, 1.

interactions) and polarization (empty/occupied orbital mixing on the same fragment). The charge transfer part is the result of both σ-donation from the ligand to the metal and π-back-donation from the metal into the unoccupied orbitals of the ligand. We used the extended transition state (ETS) method developed by Ziegler and Rauk to decompose $\Delta E^{\circ i}$ into contributions from each irreducible representation of the interacting system.[31] As the M−L bonds analyzed in this case do not exhibit a clear σ,π-separation, we can only make estimations of the contributions of σ-donation ($\Delta E_{A'} - \Delta E_{A''}$) and π-back-bonding ($2\Delta E_{A''}$) assuming near degeneracy of the ligand π^* orbitals and negligible ligand to metal π-donation.[21]

Experimental Section

General Data. All experiments were performed in flame-dried glassware and under an atmosphere of dry nitrogen or argon. Solvents were distilled (under N_2) from sodium (toluene), sodium benzophenone (THF), diphosphoruspentoxide (CH_2Cl_2, $CHCl_3$), or lithium aluminum hydride (*n*-pentane). Deuterated solvents were dried over 4 Å molecular sieves ($CDCl_3$, C_6D_6). All solid starting materials were dried in vacuo. ^{1}H, ^{13}C, and ^{31}P NMR spectra were recorded at 300 K on a Bruker Avance 250 spectrometer at 250.13, 62.90, and 101.25 MHz, respectively. ^{1}H NMR spectra were referenced to $CHCl_3$ (δ 7.27 ppm) or C_6D_5H (δ 7.17 ppm), ^{13}C NMR spectra to $CDCl_3$ (δ 77.16 ppm) or C_6D_6 (δ 128.06 ppm), and ^{31}P NMR spectra to external 85% H_3PO_4. IR spectra were recorded on a Mattson-6030 Galaxy FTIR spectrophotometer, and high-resolution mass spectra (HRMS) on a Finnigan Mat 900 spectrometer. Elemental analyses were performed by Mikroanalytisches Labor Pascher, Remagen-Bandorf, Germany. $[Cp^*RhCl_2]_2$,[36] $[CpCoI_2]_2$,[11b] $IsPH_2$,[37] and Mes^*PH_2,[38] were prepared according to literature procedures.

[Cp*RhCl$_2$(PH$_2$Mes*)] (2a). Mes^*PH_2 (0.58 g, 2.10 mmol) was added to a dark red-brown solution of $[Cp^*RhCl_2]_2$ (0.62 g, 1.00 mmol) in $CHCl_3$ (50 mL), which was stirred for 3 h at 50 °C and filtered to remove insoluble material. After concentrating the solution to ~5 mL, *n*-pentane (30 mL) was added slowly to cause precipitation of an orange-red powder, which was isolated by filtration, washed with *n*-pentane (25 mL), and dried in vacuo. Recrystallization from CH_2Cl_2/*n*-pentane yielded **2a** as red needles (1.10 g, 1.87 mmol, 94%). Mp > 240 °C (dec). ^{31}P NMR ($CDCl_3$): δ −43.1 (doublet of triplets, $^1J_{RhP}$ = 143 Hz, $^1J_{PH}$ = 387 Hz). ^{1}H NMR ($CDCl_3$): δ 1.32 (s, 15H, $C_5(CH_3)_5$), 1.34 (s, 9H, *p*-C(CH_3)$_3$), 1.55 (s, 18H, *o*-C(CH_3)$_3$), 6.38 (d, $^1J_{PH}$ = 387 Hz, 2H, PH_2), 7.48 (d, $^4J_{PH}$ = 2.5 Hz, 2H, *m*-Mes*). ^{13}C{^{1}H} NMR ($CDCl_3$): δ 9.56 (s, $C_5(CH_3)_5$), 31.6 (s, *p*-C(CH_3)$_3$), 33.6 (d, $^4J_{PC}$ = 1.9 Hz, *o*-C(CH_3)$_3$), 35.5 (s, *p*-$C(CH_3)_3$), 38.6 (d, $^3J_{PC}$ = 1.6 Hz, *o*-$C(CH_3)_3$), 99.1 (d, $^1J_{RhC}$ = 7.2 Hz, $C_5(CH_3)_5$), 116.3 (d, $^1J_{PC}$ = 24.8 Hz, *i*-Mes*), 123.0 (d, $^3J_{PC}$ = 9.4 Hz, *m*-Mes*), 152.7 (s, *p*-Mes*), 156.4 (d, $^2J_{PC}$ = 3.8 Hz, *o*-Mes*). IR (KBr, cm^{-1}): ν(PH) 2401, 2435. HRMS: calcd for $C_{28}H_{46}PCl_2Rh$ 586.17694, found 586.174664.

[Cp*RhCl$_2$(PH$_2$Is)] (2b). In a fashion similar to that described for **2a**, $IsPH_2$ (0.50 g, 2.10 mmol) was used to give orange crystals of **2b** (0.94 g, 1.72 mmol, 86%). Mp > 190 °C (dec). ^{31}P NMR ($CDCl_3$): δ −59.1 (doublet of triplets, $^1J_{RhP}$ = 141 Hz, $^1J_{PH}$ = 386 Hz). ^{1}H NMR ($CDCl_3$): δ 1.25 (d, $^3J_{HH}$ = 6.9 Hz, 6H, *p*-CH(CH_3)$_2$), 1.29 (d, $^3J_{HH}$ = 6.6 Hz, 12H, *o*-CH(CH_3)$_2$), 1.55 (d, $^4J_{PH}$ = 4.2 Hz, 15H, $C_5(CH_3)_5$), 2.89 (sep, $^3J_{HH}$ = 6.9 Hz, 1H, *p*-CH(CH$_3$)$_2$), 3.18 (sep, $^3J_{HH}$ = 6.6 Hz, 2H, *o*-CH(CH$_3$)$_2$), 5.57 (d, $^1J_{PH}$ = 386 Hz, 2H, PH_2), 7.08 (d, $^3J_{PH}$ = 3.1 Hz, 2H, *m*-Is). ^{13}C{^{1}H} NMR ($CDCl_3$): δ 9.44 (s, $C_5(CH_3)_5$), 24.2 (s, *p*-CH(CH_3)$_2$), 24.6 (s, *o*-CH(CH_3)$_2$), 33.0 (d, $^3J_{PC}$ = 9.4 Hz, *o*-$CH(CH_3)_2$), 34.8 (s, *p*-$CH(CH_3)_2$), 99.1 (dd, $^2J_{RhC}$ = 7.1 Hz, $^3J_{PC}$ = 3.3 Hz, $C_5(CH_3)_5$), 114.9 (d, $^1J_{PC}$ = 40.2 Hz, *i*-Is), 122.2 (d, $^3J_{PC}$ = 8.0 Hz, *m*-Is), 153.0 (d, $^4J_{PC}$ = 2.6 Hz, *p*-Is), 153.5 (d, $^2J_{PC}$ = 7.1 Hz, *o*-Is). IR (KBr, cm^{-1}): ν(PH) 2382, 2396. Anal. Calcd for $C_{25}H_{40}PCl_2Rh$: C, 55.06; H, 7.40; P, 5.68. Found: C, 54.68; H, 7.35; P, 5.40.

[Cp*(PPh$_3$)Rh=PMes*] (3). A red-brown solution of **2a** (117 mg, 0.20 mmol) in CH_2Cl_2 (2.5 mL) was added dropwise to a solution of DBU (59.8 μL, 0.40 mmol) and PPh_3 (52.5 mg, 0.20 mmol) in toluene (5 mL) and stirred for an additional 5 min. After removal of the solvents the residue was extracted with *n*-pentane (25 mL), filtered, and concentrated. Cooling at −20 °C yielded green-black crystals of **3** (138 mg, 0.178 mmol, 89%). Mp: 162−164 °C. ^{31}P NMR (C_6D_6): δ 867.6 (dd, $^1J_{RhP}$ = 68.6 Hz, $^2J_{PP}$ = 59.4 Hz, Rh=P), 44.1 (dd, $^1J_{RhP}$ = 239.1 Hz, $^2J_{PP}$ = 59.4 Hz, Rh−PPh_3). ^{1}H NMR (C_6D_6): δ 1.33 (d, $^4J_{PH}$ = 1.14 Hz, 15H, $C_5(CH_3)_5$), 1.50 (s, 18H, *o*-C(CH_3)$_3$), 1.51 (s, 9H, *p*-C(CH_3)$_3$), 7.04−7.20 (m, 9H, PPh_3), 7.53 (s, 2H, *m*-Mes*), 7.90 (m, 6H, PPh_3). ^{13}C{^{1}H} NMR (C_6D_6): δ 10.2 (s, $C_5(CH_3)_5$), 32.1 (d, $^4J_{PC}$ = 4.7 Hz, *o*-C(CH_3)$_3$), 32.2 (s, *p*-C(CH_3)$_3$), 35.0 (s, *p*-$C(CH_3)_3$), 38.7 (s, *o*-$C(CH_3)_3$), 97.5 (d, $^2J_{PC}$ = 4.2 Hz, $C_5(CH_3)_5$), 121.0 (s, *m*-Mes*), 127.8 (d, $^3J_{PC}$ = 9.9 Hz, *m*-PPh_3), 129.3 (d, $^4J_{PC}$ = 1.8 Hz, *p*-PPh_3), 135.5 (d, $^2J_{PC}$ = 11.3 Hz, *o*-PPh_3), 136.7 (d, $^1J_{PC}$ = 40.6 Hz, *i*-PPh_3), 144.5 (s, *o*-Mes*), 146.4 (s, *p*-Mes*). HRMS: calcd for $C_{46}H_{59}P_2Rh$ 776.31470, found 776.31745.

[Cp*(PMe$_3$)Rh=PMes*] (4). In a fashion similar to that described for **3**, **2a** (117 mg, 0.20 mmol), DBU (59.8 μL, 0.40 mmol), and PMe_3 (0.20 mL of a 1.0 M solution in toluene, 0.20 mmol) were used to give dark green crystals of **4** (93 mg, 0.158 mmol, 79%) as a mixture of isomers. Major isomer (65%) (*Z*)-**4**. ^{31}P NMR (C_6D_6): δ 953 (dd, $^1J_{RhP}$ = 86 Hz, $^2J_{PP}$ = 19 Hz, Rh=P), −6.9 (dd, $^1J_{RhP}$ = 230 Hz, $^2J_{PP}$ = 19 Hz, Rh−PPh_3). ^{1}H NMR (C_6D_6): δ 0.78 (dd, $^2J_{PH}$ = 8.5 Hz, $^4J_{PH}$ = 1.2 Hz, 9H, P(CH_3)$_3$), 1.44 (s, 9H, *p*-C(CH_3)$_3$), 1.50 (s, 18H, *o*-C(CH_3)$_3$), 1.96 (bs, 15H, $C_5(CH_3)_5$), 7.46 (bs, 2H, *m*-Mes*). Minor isomer (35%) (*E*)-**4**. ^{31}P NMR (C_6D_6): δ 815 (dd, $^1J_{RhP}$ = 66 Hz, $^2J_{PP}$ = 35 Hz, Rh=P), −14.5 (dd, $^1J_{RhP}$ = 232 Hz, $^2J_{PP}$ = 35 Hz, Rh−PPh_3). ^{1}H NMR (C_6D_6): δ 1.50 (s, 9H, *p*-C(CH_3)$_3$), 1.53 (d, $^2J_{PH}$ = 8.4 Hz, 9H, P(CH_3)$_3$), 1.53 (bs, 15H, $C_5(CH_3)_5$), 1.63 (s, 18H, *o*-C(CH_3)$_3$), 7.54 (bs, 2H, *m*-Mes*). HRMS: calcd for $C_{31}H_{53}P_2Rh$ 590.26776, found 590.26851.

[Cp*(PPh$_3$)Rh=PIs] (5). In a fashion similar to that described for **3**, **2b** (136 mg, 0.25 mmol), DBU (75 μL, 0.50 mmol), and PPh_3 (66 mg, 0.25 mmol) were used to give dark green **5** (151 mg, 0.206 mmol, 82%). The compound could not be recrystallized properly due to high solubility and therefore contains some impurities. ^{31}P NMR (C_6D_6): δ 859.5 (dd, $^1J_{RhP}$ = 63 Hz, $^2J_{PP}$ = 38 Hz, Rh=P), 45.4 (dd, $^1J_{RhP}$ = 234 Hz, $^2J_{PP}$ = 38 Hz, Rh−PPh_3). ^{1}H NMR ($CDCl_3$): 1.04 (d, $^3J_{HH}$ = 6.8 Hz, 6H, *o*-CH(CH_3)$_2$), 1.43 (d, $^3J_{HH}$ = 6.9 Hz, 6H, *p*-CH(CH_3)$_2$), 1.44 (d, $^4J_{PH}$ = 1.2 Hz, 15H, $C_5(CH_3)_5$), 1.56 (d, $^3J_{HH}$ = 6.8 Hz, 6H, *o*-CH(CH_3)$_2$), 3.02 (sep, $^3J_{HH}$ = 6.9 Hz, 1H, *p*-CH(CH$_3$)$_2$), 3.12 (sep, $^3J_{HH}$ = 6.8 Hz, 2H, *o*-CH(CH$_3$)$_2$), 7.05−7.17 (m, 9H, PPh_3), 7.22 (s, 2H, *m*-Is), 7.90−7.95 (m, 6H, PPh_3). ^{13}C{^{1}H} NMR ($CDCl_3$): 9.7 (s, $C_5(CH_3)_5$), 23.2 (s, *p*-CH(CH_3)$_2$), 24.8 (s, *o*-CH(CH_3)$_2$), 24.9 (s, *o*-CH(CH_3)$_2$), 31.4 (bs, *o*-$CH(CH_3)_2$), 35.0 (s, *p*-$CH(CH_3)_2$), 97.0 (dd, $^1J_{RhC}$ = 4.2 Hz, $^2J_{PC}$ = 3.0 Hz, $C_5(CH_3)_5$), 119.7 (s, *m*-Is), 127.6 (d, $^3J_{PC}$ = 9.7 Hz, *m*-PPh_3), 129.3 (d, $^4J_{PC}$ = 2.0 Hz, *p*-PPh_3), 135.5 (d, $^2J_{PC}$ = 11.4 Hz, *o*-PPh_3), 137.0 (d, $^1J_{PC}$ = 39.9 Hz, *i*-PPh_3), 143.6 (s, *p*-Is), 147.2 (s, *o*-Is). HRMS: calcd for $C_{43}H_{53}P_2Rh$ 734.26776, found 734.26837.

[CpCoI$_2$(PH$_2$Mes*)] (7). To a suspension of $[CpCoI_2]_n$ (1.0 g, 2.65 mmol) in CH_2Cl_2 (25 mL) was added a solution of Mes^*PH_2 (0.75 g, 2.70 mmol) in CH_2Cl_2 (5 mL). The resulting dark green mixture was stirred for 1 h at room temperature, after which it was filtered and concentrated to a few milliliters. Subsequent addition of *n*-pentane and cooling to 0 °C caused formation of a green-black precipitate that was isolated by filtration, washed with cold *n*-pentane, and dried in vacuo (1.36 g, 2.07 mmol, 78%). The solid is stable, but in solution, **7** slowly decomposes, which hampers further purification by crystal-

(36) White, C.; Yates, A.; Maitlis, P. M. *Inorg. Synth.* **1992**, *29*, 228.
(37) van den Winkel, Y.; Bastiaans, H. M. M.; Bickelhaupt, F. *J. Organomet. Chem.* **1991**, *405*, 183.
(38) Cowley, A. H.; Kilduff, J. E.; Newman, T. H.; Pakulski, M. *J. Am. Chem. Soc.* **1982**, *104*, 5820.

lization. Mp > 140 °C (dec). ^{31}P NMR ($CDCl_3$): δ −48.9 (bt, $^1J_{PH}$ = 382 Hz). ^{1}H NMR ($CDCl_3$): δ 1.34 (s, 9H, *p*-C(CH_3)$_3$), 1.71 (s, 18H, *o*-C(CH_3)$_3$), 4.85 (s, 5H, C_5H_5), 7.06 (d, $^1J_{PH}$ = 382 Hz, 2H, PH_2), 7.59 (d, $^4J_{PH}$ = 2.9 Hz, 2H, *m*-Mes*). ^{13}C NMR ($CDCl_3$): δ 30.9 (s, *p*-C(*C*H_3)$_3$), 33.6 (s, *o*-C(*C*H_3)$_3$), 35.2 (s, *p*-*C*(CH$_3$)$_3$), 38.4 (d, $^3J_{CP}$ = 2.3 Hz, *o*-*C*(CH$_3$)$_3$), 85.2 (d, $^2J_{CP}$ = 3.3 Hz, C_5H_5), 122.0 (d, $^1J_{PC}$ = 30 Hz, *i*-Mes*), 123.5 (d, $^3J_{PC}$ = 9.8 Hz, *m*-Mes*), 152.8 (s, *p*-Mes*), 154.7 (d, $^2J_{PC}$ = 5.3 Hz, *o*-Mes*). IR (KBr, cm^{-1}): ν(PH) 2375, 2346.

[Cp(PPh$_3$)Co=PMes*] (8). A dark green solution of [Cp(PH$_2$Mes*)CoI$_2$] (**7**; 328 mg, 0.50 mmol) in CH_2Cl_2 (2.0 mL) was added slowly to a stirred solution of DBU (150 μL, 1.00 mmol) and PPh_3 (131 mg, 0.50 mmol) in toluene (5 mL) at 0 °C. The resulting dark red solution was warmed to room temperature and stirred for an additional 5 min. After removal of the solvents, the residue was extracted into *n*-pentane (25 mL), filtered, and concentrated. Crystallization at −20 °C yielded dark red crystals of **8**·C_5H_{12} (153 mg, 0.21 mmol, 42%). Mp: 83−84 °C. ^{31}P NMR (C_6D_6): δ 866.9 (d, $^2J_{PP}$ = 76 Hz, Co=P), 54.0 (bd, $^2J_{PP}$ = 76 Hz, PPh_3). ^{1}H NMR (C_6D_6): δ 1.49 (s, 18H, *o*-C(CH_3)$_3$), 1.55 (s, 9H, *p*-C(CH_3)$_3$), 4.12 (s, 5H, C_5H_5), 7.07−7.15 (m, 9H, PPh_3), 7.64 (s, 2H, *m*-Mes*), 7.86−7.94 (m, 6H, PPh_3). ^{13}C NMR (C_6D_6): δ 31.8 (s, *p*-C(*C*H_3)$_3$), 31.9 (bs, *o*-C(*C*H_3)$_3$), 35.2 (s, *p*-*C*(CH$_3$)$_3$), 38.8 (s, *o*-*C*(CH$_3$)$_3$), 82.2 (d, $^2J_{PC}$ = 2.1 Hz, C_5H_5), 121.0 (s, *m*-Mes*), 128.8 (d, $^3J_{PC}$ = 9.4 Hz, *m*-PPh_3), 129.4 (d, $^4J_{PC}$ = 2.1 Hz, *p*-PPh_3), 134.8 (d, $^2J_{PC}$ = 10.5 Hz, *o*-PPh_3), 137.5 (d, $^1J_{PC}$ = 40.1 Hz, *i*-PPh_3), 144.4 (d, $^2J_{PC}$ = 0.6 Hz, *o*-Mes*), 147.4 (s, *p*-Mes*), 171.3 (dd, $^1J_{PP}$ = 105.7 Hz, $^3J_{PP}$ = 19.4 Hz, *i*-Mes*). HRMS: calcd for $C_{41}H_{49}P_2Co$ 662.26416, measd 662.26489.

Reaction of Phosphinidene Complexes 3 and 8 with CH_2X_2 and CHX_3 on an NMR Scale. A small excess of CH_2X_2 (0.12 mmol) was added to a dark green solution of **3** (0.10 mmol) in *n*-pentane (0.5 mL), and the reaction was followed by ^{31}P NMR spectroscopy for product formation. An orange-red precipitate of Cp*(PPh_3)RhX_2 formed quantitatively over a period of 1 h (I), 12 h (Br), and 48 h (Cl) at room temperature and was removed by decanting the solution and washing the residue twice with *n*-pentane (1 mL). The combined *n*-pentane solutions were evaporated to yield Mes*P=CH_2 as a yellow solid. Performing the reaction with CHI_3 resulted in the quantitative formation of orange-colored Mes*P=CHI as a mixture of *E* (14%) and *Z* (86%) isomers. ^{31}P, ^{1}H, and ^{13}C NMR are as reported in the literature.[39] The reactions were performed in a similar fashion for **8**.

X-ray Crystal Structure Determinations of 3 and 8. Intensities were measured on a Nonius KappaCCD diffractometer with a rotating anode (Mo Kα, λ = 0.71073 Å) at a temperature of 150(2) K. The structures were solved with direct methods (SIR-97)[40] and refined with the program SHELXL-97[41] against F^2 of all reflections. Non hydrogen atoms were refined freely with anisotropic displacement parameters. Hydrogen atoms were refined freely with isotropic displacement parameters (compound **3**) or as rigid groups (compound **8**). The drawings, structure calculations, and checking for higher symmetry was performed with the program PLATON.[42]

Compound 3: $C_{46}H_{59}P_2Rh$, fw = 776.78, dark green prism, 0.25 × 0.25 × 0.13 mm^3, triclinic, space group $P\bar{1}$ (no. 2). Cell parameters: a = 9.7539(1) Å, b = 14.3652(2) Å, c = 16.8717(2) Å, α = 64.9564(7)°, β = 78.5027(7)°, γ = 72.6990(7)°, V = 2037.47(4) Å^3. Z = 2, ρ = 1.266 g cm^{-3}, $F000$ = 820. 38 294 reflections were measured up to a resolution of (sin θ/λ) = 0.65 Å^{-1}; 9302 reflections were unique (R_{int} = 0.0637). An absorption correction based on multiple measured reflections was applied (μ = 0.528 mm^{-1}, 0.71−0.93 transmission). 678 refined parameters, no restraints. R (obs reflns): R1 = 0.0281, wR2 = 0.0702. R (all data): R1 = 0.0326, wR2 = 0.0728. Weighting scheme $w = 1/[\sigma^2(F_o^2) + (0.0310P)^2 + 0.9560P]$, where $P = (F_o^2 + 2F_c^2)/3$. GoF = 1.030. Residual electron density between −0.64 and 0.54 e/Å^3.

Compound 8: $C_{41}H_{49}CoP_2$·C_5H_{12}, fw = 734.82, red plate, 0.27 × 0.27 × 0.09 mm^3, monoclinic, space group $P2_1/c$ (no. 14). Cell parameters: a = 17.4679(4) Å, b = 11.2656(3) Å, c = 26.2346(5) Å, β = 125.8431(10)°, V = 4184.93(17) Å^3. Z = 4, ρ = 1.166 g cm^{-3}, $F000$ = 1576. 26 578 reflections were measured up to a resolution of (sin θ/λ) = 0.59 Å^{-1}; 7314 reflections were unique (R_{int} = 0.0654). An absorption correction was not considered necessary. The pentane solvent molecule was refined with a disorder model and with isotropic displacement parameters. 438 refined parameters, 43 restraints. R (obs reflns): R1 = 0.0443, wR2 = 0.0984. R (all data): R1 = 0.0775, wR2 = 0.1108. Weighting scheme $w = 1/[\sigma^2(F_o^2) + (0.0474P)^2 + 1.8625P]$, where $P = (F_o^2 + 2F_c^2)/3$. GoF = 1.011. Residual electron density between −0.33 and 0.53 e/Å^3.

Acknowledgment. This work was supported by The Netherlands Foundation for Chemical Sciences (CW) with financial aid from the Netherlands Organization for Scientific Research (NWO). Dr. H. Zappey is acknowledged for measuring high-resolution mass spectra.

Supporting Information Available: Cartesian coordinates of the optimized structures. Crystallographic data for compounds **3** and **8**. This material is available free of charge via the Internet at http://pubs.acs.org.

OM0208624

(39) Appel, R.; Casser, C.; Immenkeppel, M.; Knoch, F. *Angew. Chem.* **1984**, *96*, 905; *Angew. Chem., Int. Ed. Engl.* **1984**, *23*, 895. (b) Appel, R.; Immenkeppel, M. *Z. Anorg. Allg. Chem.* **1987**, *553*, 7. (c) Goede, S.; Bickelhaupt, F. *Chem. Ber.* **1991**, *124*, 2677.

(40) Altomare, A.; Burla, M. C.; Camalli, M.; Cascarano, G. L.; Giacovazzo, C.; Guagliardi, A.; Moliterni, A. G. G.; Polidori, G.; Spagna, R. *J. Appl. Crystallogr.* **1999**, *32*, 115.

(41) Sheldrick, G. M. *SHELXL-97*, Program for crystal structure refinement; University of Göttingen: Germany, 1997.

(42) Spek, A. L. *PLATON*, a multipurpose crystallographic tool; Utrecht University: The Netherlands, 2001.